

Questions and Answers

Chapter 11

Questions

- (Q1) *What is the essence of the chapter?*
- (Q2) *What are the two main areas used in this chapter when it comes to X-ray breast imaging?*
- (Q3) *What are the different measures used for X-ray breast “contrast enhancement”? Discuss each of them.*
- (Q4) *Show how the knowledge-based system works for the contrast enhancement.*
- (Q5) *What is the role of image segmentation here and how it is done?*
- (Q6) *What is double network mapping (DNM)?*
- (Q7) *What is breast profile mapping (BPM)? Discuss in detail.*
- (Q8) *Discuss the weighted GMM/MRF model of segmentation of breast masses in X-ray images. State mathematically and then discuss the pseudo algorithm.*
- (Q9) *Compare the four models ($WGMM_S$, $WGMM_U$, $WGMM_S^{MRF}$, $WGMM_U^{MRF}$).*
- (Q10) *List some key observations in adaptive knowledge-based model.*

Answers

- (A1) This chapter introduces the concept of a knowledge-based approach to medical imaging. This involves an adaptive framework within which operations such as image enhancement, segmentation, feature extraction and classification, and false positive reduction are calculated. The framework is adaptive since it modifies the parameters of the various tools used in different layers of analysis depending on the properties of the image analyzed. In particular, the results are shown in the area of digital mammography; however, the proposed framework is generic in that it is independent of the application area or the tools used.
- (A2) The two main areas are (1) contrast enhancement of breast X-ray images and (2) segmentation of masses (lesions or cancerous zones) in X-ray breast images.
- (A3) The following are the contrast enhancement measures used in this chapter:
- (a) Distribution separation measure (DSM)
 - (b) Combined measure based on target to background contrast enhancement measurement using entropy and target to background contrast enhancement measurement based on standard deviation (TBC_s).
 - (c) Difference in average separation measure

(a) Distribution separation measure (DSM)

Using the method for labeling the Target (T) and Background (B) regions, it is possible to plot the overlap of the density functions for the gray scales comprising these two regions. In mammography, this is representative of the overlap found between a breast cancer lesion and its background border. A good enhancement technique should ideally reduce the overlap. In particular, it is anticipated that the enhancement technique should help reduce the spread of the target distribution and shift its mean gray-scale level to a higher value thus separating the two distributions and reducing their overlap. The best decision boundary for the original image between the two classes, assuming both classes have a multivariate

normal distribution with equal covariances, is given using [21] as

$$D_1 = \frac{\mu_B^O \cdot \sigma_T^O + \mu_T^O \cdot \sigma_B^O}{\sigma_T^O \cdot \sigma_B^O} \quad (11.1)$$

Similarly, the best decision boundary for the original image after enhancement is given as

$$D_2 = \frac{\mu_B^E \cdot \sigma_T^E + \mu_T^E \cdot \sigma_B^E}{\sigma_T^E \cdot \sigma_B^E} \quad (11.2)$$

where μ_B^O , σ_B^O , μ_T^O , and σ_T^O are the mean and standard deviation of the gray scales comprising the background and target area, respectively, of the original image before enhancement. Similarly μ_B^E , σ_B^E , μ_T^E , and σ_T^E correspond to the mean and standard deviation of the gray scales after the enhancement. An alternative approximation to D_1 and D_2 can be found using the cutting score [22]. If the groups are assumed to be representative of the population, a weighted average of the group centroids will provide an optimal cutting score where Eq. (11.1) is rewritten as

$$D_1 = \frac{\mu_B^O \cdot N_T^O + \mu_T^O \cdot N_B^O}{N_T^O \cdot N_B^O} \quad (11.3)$$

and Eq. (11.2) is rewritten as

$$D_2 = \frac{\mu_B^E \cdot N_T^E + \mu_T^E \cdot N_B^E}{N_T^E \cdot N_B^E} \quad (11.4)$$

where N_B^O and N_T^O are the number of samples in the background and target prior to enhancement, and N_B^E and N_T^E the respective sample numbers after the enhancement. Again this approximation assumes that the two distributions are normal and that the group dispersion structures are known. By combining Eqs. (11.3) and (11.4) it is possible to compute a distance measure between the decision boundaries and the means of the targets and background, before and after segmentation. This measure is termed as the distribution separation measure (DSM) and it is a measure of the quality of enhancement. It is defined as

$$\text{DSM} = \{ |(D_2 - \mu_B^E)| + |(D_2 - \mu_T^E)| \} - \{ |(D_1 - \mu_B^O)| + |(D_1 - \mu_T^O)| \} \quad (11.5)$$

Ideally the measurement should be greater than zero; the greater the DSM value, the better the quality of enhancement. For comparing any two enhancement techniques, choose the technique that gives a higher value on the DSM measure.

(b) Combined method

Target to background contrast enhancement measurement based on standard deviation (TBC_s)

A key objective of a contrast enhancement is to maximize the difference between background and target mean gray level and ensure that the homogeneity of the mass is increased aiding the visualization of its boundaries and location. Using the ratio of the standard deviation of the gray scales within the target before and after the enhancement, the improvement using the target to background contrast enhancement using standard deviation (TBC_s) is given as

$$TBC_s = \left\{ \frac{(\mu_T^E/\mu_B^E) - (\mu_T^O/\mu_B^O)}{\sigma_T^E/\sigma_T^O} \right\} \quad (11.6)$$

where the mean and standard deviation of the gray scales comprise the target and background before and after the enhancement. Assuming that the target has a smaller mean before and after enhancement compared to the background, it is expected that as a result of enhancement, this measure should give a value greater than zero.

Target to background contrast enhancement measurement based on entropy (TBC_ε)

It is possible to extend the concept of (TBC_s) further by replacing the standard deviation with the entropy of the target in the original and enhanced images, ε_T^O and ε_T^E , respectively, to quantify the homogeneity ratio. Similar to Eq. (11.6), the target to background contrast enhancement using entropy (TBC_ε) is defined as

$$TBC_\varepsilon = \left\{ \frac{(\mu_T^E/\mu_B^E) - (\mu_T^O/\mu_B^O)}{\varepsilon_T^E/\varepsilon_T^O} \right\} \quad (11.7)$$

Assuming that the target has a smaller mean before and after enhancement compared to the background, it is expected that as a result of enhancement, this measure should give a value greater than zero.

The combined enhancement measure (D)

It is possible to combine the three novel measures into a single quantitative value. Using this combined measure, a researcher is able to quantitatively rank enhancements for a particular image. To combine DSM, TBC_s , and TBC_e for a particular enhancement, each enhancement value is represented within a 3-D Euclidean space by min-max scaling each within the range $[0, 1]$. A high performance contrast enhancement method will have points close to coordinates $(1, 1, 1)$. The combined measure D is computed by calculating the Euclidean distance between the point in the 3-D coordinate space representing the enhancement and $(1, 1, 1)$. This point in the enhancement measurement space represents the location of an enhancement method that results in the maximal increase in contrast between a target and its background. The combined measure D is computed as

$$D = \sqrt{(1 - \text{DSM})^2 + (1 - TBC_s)^2 + (1 - TBC_e)^2} \quad (11.8)$$

The enhancement method giving the smallest value of D is selected as the best enhancement method for this image.

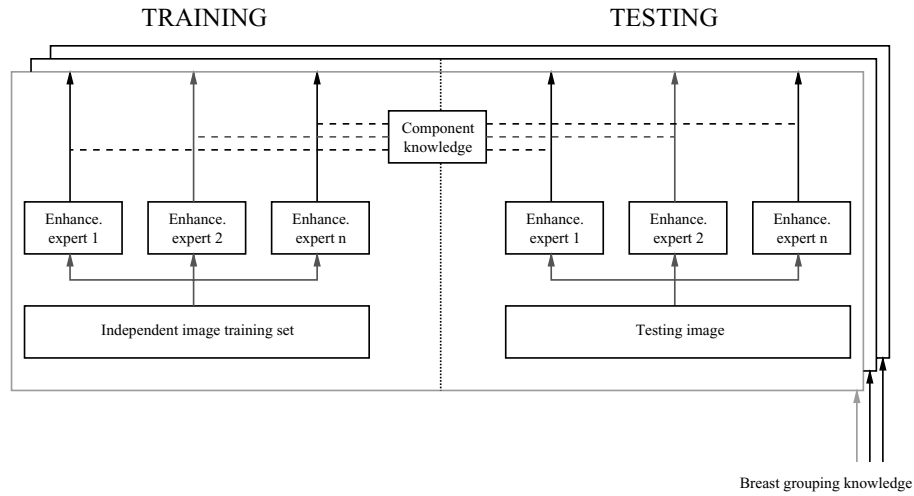
(c) Difference in average separation measure AVS_{diff}

This measure is defined as the difference in average separation (AVS) [23] between the original and corresponding enhanced image. The average separation is a measure of intergroup dissimilarity and is defined as the average Euclidean distance d between “confused pixels,” that is, pixels with the same gray scales found in both target and background regions. The AVS measure is defined as

$$AVS(\omega_1, \omega_2) = \frac{1}{n_1 n_2} \sum_{i=1}^{n_1} \sum_{j=1}^{n_2} d(x_i, y_j) \quad x_i \in \omega_1, \quad x_j \in \omega_2 \quad (11.9)$$

for all pairs of points such that a single point is drawn from each region, target ω_1 and background ω_2 with n_1 and n_2 pixels in total respectively. A large value of AVS_{diff} will result if the enhanced image has a greater intergroup dissimilarity for gray scales in the target and background region compared with that of the original. This increased value of $AVS_{enhanced}$ indicates that the enhancement has maximized the Euclidean distance of the confused pixels thereby resulting in an improved contrast enhancement.

(A4)



(A5) The aim of image segmentation is to label a pixel in an image as belonging to one of the known corresponding real world objects. In the detection of breast lesions in digitized mammograms, image segmentation results in contiguous areas or regions of pixels, labeled as normal or suspicious. For the purpose of evaluating image enhancement, we use an unsupervised Gaussian mixture model (GMM) and hidden Markov random field ($HMRF_U$) model of image segmentation proposed by Zhang *et al.* [24]. For ease of referencing, this shall be referred to as $HMRF_U$ in the rest of this chapter. The $HMRF_U$ segmentation method is used to segment contrast-enhanced images so that the performance of the contrast enhancement can be determined. The $HMRF_U$ segmentation algorithm operates in an unsupervised manner. The only *a priori* knowledge required for the

segmentation is the maximum number of classes, L , from which a pixel is labeled. By setting $L = 2$, HMRF_U will label pixels as either normal or suspicious. The HMRF_U method models each class using a single Gaussian whose parameters are defined using a maximum likelihood estimate. Following convergence, a maximum a posteriori (MAP) segmentation is performed by labeling each pixel with the class maximizing the a posteriori probability estimates.

- (A6) This strategy adopts a divide-and-conqueror paradigm. It attempts to decompose a single mapping into two simpler mappings. The first mapping to be learnt between the features from ROI and the three quantitative measure of enhancement performance proposed in section 11.3.1. A second process learns the mapping of the quantitative measure of enhancement with quantitative measure of segmentation. On testing this strategy will predict a measure of segmentation for each contrast enhancement method, and the actual contrast enhancement method is identified as the one maximizing the segmentation performance.
- (A7) The second strategy used for learning the expert contrast enhancement for a mammogram is the breast profile mapping (BPM) strategy. For a mammogram I , enhanced using enhancement method E_m where $m \in \{1, \dots, M\}$, the BPM strategy learns the mapping between the set of N gray scale input features F_{BP^N} detailed in section 11.3.3.1 and a $l = \{1, \dots, L\}$ indicates the target contrast enhancement for a training mammogram. Both feature sets $\{F_{BP^{316}}, F_{BP^{26}}\}$ are evaluated separately in their utility for learning the expert contrast enhancement. The expert l is based on a set of R measures quantifying the performance of lesion segmentation $S = \{s_1, s_2, \dots, s_R\}$ described in Table 11.2. The expert l is identified as the one maximizing the sum of TP^T and $SUBTP^T$ outcomes for each enhancement method E_m where $m \in \{1, \dots, M\}$ as defined previously in Eq. (11.10). Unlike the DNM strategy, this method utilizes a single classifier to predict the target contrast enhancement method. The k -nearest neighbor (k -NN) classifier has been show to be effective at learning nonparametric mappings with a small sample size [27] and for this reason it is employed in the knowledge-based contrast enhancement expert. To evaluate the strategy a fivefold cross validation is used to reduce bias and provide a test decision for each mammogram.

Training the BPM approach

To train the BPM strategy, the set of gray-scale input features $F_{BP^N} = (f_1, f_2, \dots, f_N)$, where N identifies the original and PCA feature sets ($N = \{316, 26\}$), are extracted from the segmented breast profile. Each training mammogram is contrast enhanced with each enhancement method. The quantitative measures of segmentation are calculated for the target ROI. For each enhancement method, the winning predicted enhancement method identified by the label l is used to learn the mapping between F and l with the k -NN classifier.

Testing the BPM approach

To determine the predicted target enhancement method E_l for a test mammogram I , the set of gray-scale input features F_{BP^N} are extracted from the segmented breast profile. Using the trained k -NN classifier, the predicted actual expert contrast enhancement is determined.

Model order selection

In order that the BPM strategy is to perform optimally, the number of nearest neighbors k , must be correctly set. For each input feature set $F_{BP^{316}}$ and $F_{BP^{26}}$ for different values of k the validation set error is plotted and the value of k corresponding to the least error is chosen.

BPM framework results

Feature set $F_{BP^{316}}$: Using an optimized value of $k = 23$, Table 11.7 shows the percentage improvement in segmentation performance when using the predicated actual enhancement method, compared with that obtained with the unenhanced original, from the $F_{BP^{316}}$ set. These results show that the segmentation improvement obtained over the unenhanced image, when segmenting an image enhanced using a enhancement method predicted by the BPM strategy, is greater than that obtained using the DNM strategy predicted enhancement method. However, segmenting the BPM strategy's predicted enhanced image results in inferior performance to that using the target enhancement method identified in Table 11.4. The result for breast type 4, the densest breast type shows a small improvement over using the FUZZY method, shown in Table 11.5(part c), for all mammograms of that type.

Feature set $F_{BP^{26}}$: Using an optimized value of $k = 19$, Table 11.8 shows the percentage improvement in segmenting the unenhanced image

compared to that when segmenting the image enhanced using the using predicted enhancement method by the optimized BPM strategy with the $F_{BP^{26}}$ feature set. These results indicate better performance than the DNM strategy but are still inferior to the segmentation using the target expert enhancement method shown in Table 11.4. The result for breast type 1–3 show an improvement over using the FUZZY method in Table 11.5(part c) for all mammograms of that type. Comparing the results from the evaluation of the two feature sets, $F_{BP^{26}}$ and $F_{BP^{316}}$ from the BPM strategy, the results indicate that the feature set $F_{BP^{26}}$ is better suited to processing mammograms with breast types 1–3 whereas the feature set $F_{BP^{316}}$ gives better performance on the densest breast type, i.e. type 4. Interestingly, for both feature sets, the performance improvement is worse over the fattiest breast types, type 1, compared with the densest, type 4. This is because of the variability of optimal enhancement method for the fatty breast types, whereas the denser breasts tend to be optimal enhanced by the FUZZY method more often.

- (A8) A finite mixture model (FMM) [23, 27, 32] is defined as a linear combination of M component conditional densities $f(x|m, \theta_m)$, for $m = \{1, \dots, M\}$, and M mixing coefficients $f(m)$ of the form:

$$f(x) = \sum_{m=1}^M f(m) f(x|m, \theta_m) \quad (11.14)$$

such that the mixing coefficients $f(m)$ satisfy the following constraints:

$$\sum_{m=1}^M f(m) = 1 \quad \text{and} \quad 0 \leq f(m) \leq 1.$$

The framework of WGMM comprises of $l \in (1, \dots, L)$ class densities each modeled independently using a GMM of the form given in Eq. (11.14) and a set of mixing coefficients $p(\omega_l)$ as

$$p(x) = \sum_{l=1}^L p(\omega_l) p(x|\omega_l, \Theta_l) \quad (11.15)$$

The l th GMM estimates the class-conditional *pdf*, $p(x|\omega_l, \Theta_l)$ which is itself another mixture model, for each data point for each class $\{\omega_l\}_{l=1}^L$. The vector Θ_l is defined as the M component Gaussian parameters of the l th GMM as $\Theta_l = \{P_l(m), \mu_{lm}, \sum_{lm}\}$, $\forall m = \{1, \dots, M\}$. Each estimate of the class conditional *pdf* is mixed to model the overall unconditional

density $p(x)$, using a mixing coefficient $p(\omega_l)$, identifying the contribution of the l th class density in the unconditional *pdf*.

If it is assumed that for a complete dataset X , of points x_n , where $X \equiv \{x_1, \dots, x_N\}$ is drawn independently from the distribution $f(x|\theta)$, then the joint occurrence of the whole dataset can be conveniently expressed as the log likelihood as follows:

$$\log \zeta(\Theta) = \sum_{n=1}^N \log p(x_n | \Theta) = \sum_{n=1}^N \log \sum_{l=1}^L \gamma_{nl} p(\omega_l) p(x_n | \omega_l, \Theta_l) \quad (11.16)$$

Using a modified version of the expectation-maximization (EM) algorithm, as described below, we derive an ML estimate of the parameter values of each of the L GMMs $\{\Theta_l\}_{l=1}^L$.

The general framework for parameter estimation in GMM can be used to learn the parameters of WGMM. Here the component conditional densities, appearing in Eq. (11.13) are themselves mixture models. In the EM algorithm, the update equations for mixing coefficients do not depend on the functional particulars of the component densities. Hence, the mixing coefficients of the WGMM are updated according to

$$P^{\text{new}}(\omega_l) = \frac{1}{N} \sum_{n=1}^N p^{\text{old}}(\omega_l | x_n, \Theta_l^{\text{old}}) \quad (11.17)$$

The m -step involves maximizing the auxiliary function with respect to the parameters $\{\Theta_l\}_{l=1}^L$. The auxiliary function can be written as

$$Q(\Theta^{\text{new}}, \Theta^{\text{old}}) = \sum_{n=1}^N \sum_{l=1}^L p^{\text{old}}(\omega_l | x_n, \Theta_l^{\text{old}}) \log P^{\text{new}}(\omega_l) p^{\text{new}}(x_n | \omega_l, \Theta_l^{\text{new}}) \quad (11.18)$$

where

$$p^{\text{new}}(x_n | \omega_l, \Theta_l^{\text{new}}) = \sum_{m=1}^M P^{\text{new}}(m_l) p^{\text{new}}(x_n | m_l, \Theta_{ml}^{\text{new}}) \quad (11.19)$$

Writing $\gamma_{nl} = p^{\text{old}}(\omega_l | x_n, \Theta_l^{\text{old}})$, the auxiliary function can be written as the sum of L auxiliary functions, one for each mixture model:

$$Q(\Theta^{\text{new}}, \Theta^{\text{old}}) = \sum_{n=1}^N \sum_{l=1}^L \gamma_{nl} \log P^{\text{new}}(\omega_l) p^{\text{new}}(x_n | \omega_l, \Theta_l^{\text{new}}) \quad (11.20)$$

$$Q(\Theta^{\text{new}}, \Theta^{\text{old}}) = \sum_{l=1}^L \hat{Q}_l(\Theta^{\text{new}}, \Theta^{\text{old}}) \quad (11.21)$$

$$\text{where } \gamma_{nl} = p(\omega_l | x_n, \Theta_l) = \frac{p(x_n | \omega_l, \theta_l) P(\omega_l)}{\sum_{j=1}^L p(x_n | \omega_j, \theta_j) P(\omega_j)} \quad (11.22)$$

$$\text{and } \hat{Q}_l(\Theta_l^{\text{new}}, \Theta_l^{\text{old}}) = \sum_{n=1}^N \gamma_{nl} \log P^{\text{new}}(\omega_l) p^{\text{new}}(x_n | \omega_l, \theta_l^{\text{new}}) \quad (11.23)$$

The procedure for maximizing the overall likelihood of a WGMM is outlined in Algorithm 1. It consists of an outer EM loop, which are nested in L inner EM loops. Each time the outer loop is traversed, the mixing weights $p(\omega_l)$ are updated according to Eq. (11.17) and the L inner loops are iterated to update the mixing weights $p_l(m)$, means μ_{lm} , and covariances Σ_{lm} for each of the components. It should be noted that it is not necessary to iterate the inner loops to converge on each outer EM step, since it is only necessary to increase the auxiliary function to ensure convergence of the overall likelihood to a local maximum.

Pseudo Algorithm 1: WGMM Algorithm

1. Make an initial estimate of all GMM parameter values $\{\Theta_l\}_{l=1}^L$ and $p(\omega_l)$.
 2. **Iterate** outer E -step and outer M -step until the change in auxiliary function (Eq. 11.18) between iterations is less than some convergence threshold $\text{WGMM}_{\text{converge}}$.
 3. **Outer EM E-step:**
 - (a) Compute $\gamma_{nl} = p^{\text{old}}(\omega_l | x_n, \Theta_l^{\text{old}})$.
 - (b) Evaluate an auxiliary function $Q(\Theta^{\text{new}}, \Theta^{\text{old}})$ as in Eq. (11.18).
 4. **Outer EM M-step:**
 - (a) **Inner EM-steps**
For each GMM modeling the class-conditional *pdf* of classes $\omega_l = \{1, \dots, L\}$ do (Update the parameter values of each individual GMM using the GMM-EM algorithm until convergence).
 - (b) Find new values for the WGMM mixing coefficients, Θ^{new} , that maximizes the auxiliary function given in step 3(b) above.
 5. Iterate steps 2–4 until the convergence criteria is satisfied.
-

Finally, we combine our WGMM model with MRF in the same manner as Zhang *et al.* [24] combined GMM with MRF. The WGMM^{MRF} model is based on Eq. (11.15) except that the mixing coefficients $p(\omega_l)$ are replaced

with a MRF-MAP estimate $p(y_n = \omega_l | \mathfrak{s}_n)$ using ICM algorithm [29]. The auxiliary function given in Eq. (11.17) is rewritten to include the MRF hidden model as follows:

$$Q(\Theta^{\text{new}}, \Theta^{\text{old}}) = \sum_{n=1}^N \sum_{l=1}^L p^{\text{old}}(\omega_l | x_n, \Theta_l^{\text{old}}) \times \log(p(y_n = \omega_l | \mathfrak{s}_n) p^{\text{new}}(x_n | \omega_l, \theta_l^{\text{new}})) \quad (11.24)$$

The update equations for the mean and covariances in the GMM-EM algorithm remain unchanged. The MRF-MAP estimate is combined in the conditional density function $p^{\text{old}}(\omega_l | x_n, \theta_l^{\text{old}})$ as

$$\gamma_{nl} = p(\omega_l | x_n, \theta_l) = \frac{p(x_n | \omega_l, \Theta_l) p(y_n = \omega_l | \mathfrak{s}_n)}{\sum_{j=1}^M p(x_n | \omega_j, \Theta_j) p(y_n = \omega_j | \mathfrak{s}_n)} \quad (11.25)$$

The WGMM^{MRF}-EM algorithm is used to determine the ML estimates of the parameter values by iterating the WGMM-EM algorithm while constraining the density estimation with the hidden MRF model. For supervised learning, the labeled training data is used for the initialization of the WGMM and WGMM^{MRF} models, to give us WGMM_S and WGMM_S^{MRF}, and no training data is used for the unsupervised learning case, WGMM_U and WGMM_U^{MRF}.

- (A9) A cross-validation approach is used to determine the optimal number of component Gaussians, for each breast type. The determined value of m is then used for all training folds comprising each breast type. To determine the optimal value of m , models with a different number of components are trained and evaluated with a WGMM_S strategy, using an independent validation set. Model fitness is quantified by examining the log likelihood resulting from the validation set. Training files are created by taking 200 samples randomly drawn with replacement from each normal and abnormal images for each breast type. For training we use 50 training images per breast type ($n = 25$ normal, $n = 25$ abnormal) giving a training size of 10,000 samples per breast type. Repeating the procedure for 50 remaining validation image per breast type, we get 10,000 samples for validation.

In our evaluation procedure the aim is to determine the correct number of true positives (TP), false positives (FP), true negatives (TN), and false negatives (FN) in order to plot the ROC curve. A detailed

summary of how each segmented region is classed as one of these is detailed in [18]. The results are shown in Table 11.10 grouped on the basis of breast density. It is easily concluded that the supervised strategy with MRF is a clear winner. Interestingly, the performance of this method is superior for denser images compared to fatty ones. A simple explanation for this phenomenon could be based on the model order selection where $m = 1$ for the abnormal class of the fatty breast types. A more sophisticated approach to determining model order might improve the segmentation of these breast types. Without the hidden MRF model, the supervised strategy is inferior to the unsupervised approach on the denser breasts.

(A10) This section has presented a configuration of the adaptive knowledge-based model. The performance of the model has been evaluated on a dataset of 200 abnormal mammograms from four different breast types. The aim of the evaluation has been to demonstrate the utility of the model compared with that of individual experts. Following this, the performance of a specific configuration of the adaptive knowledge-based model has been evaluated on a dataset of 400 mammograms, comprising 200 abnormal and 200 normal images. From these evaluations, the following key observations can be made:

1. *Utility of knowledge-based contrast enhancement component:* Using a dataset of 200 abnormal mammograms, the utility of the knowledge-based contrast enhancement expert has been demonstrated to be greater than that of the best performing expert contrast enhancement method. Using the predicted optimal contrast enhancement method in image segmentation results in a 60% improvement in the detection of abnormal regions over the original segmentation. This is compared to a 54% improvement from the single best performing expert, the FUZZY contrast enhancement method.
2. *Utility of knowledge-based segmentation component:* By optimally combining the segmentation outcomes of 10 different segmentation experts, each operating on a unique feature space partition, the knowledge-based segmentation component resulted in a mean ROC A_z value of 0.72 for 200 mammograms from four breast types. This is compared to the best performing gray-scale segmentation expert reporting a mean A_z value of 0.65.

3. *Utility of adaptive knowledge-based model in presence of normal mammograms:* Evaluation of the performance of this configuration of the adaptive knowledge-based model on a dataset of 400 mammograms comprising 200 abnormal and 200 normal images results in a segmentation sensitivity of 0.84 for the detection of breast lesion with 167.01 false-positive regions per image. This demonstrates a high level of sensitivity in the presence of a complete spectrum of mammogram types.

4. *False-positive reduction:* The results following region prefiltering in the false-positive reduction methodology demonstrate the utility of the region size thresholding strategy. Following classification by each trained optimized artificial neural network (ANN) results in a sensitivity of 0.75 with 6.46 false-positive regions per image.